Journal of Power Sources 223 (2013) 319–324

Contents lists available at SciVerse ScienceDirect

Journal of Power Sources

journal homepage: www.elsevier.com/locate/jpowsour

Carbon electrode with perovskite-oxide catalyst for aqueous electrolyte lithium-air secondary batteries

Hirokazu Ohkuma, Ichiro Uechi, Nobuyuki Imanishi*, Atsushi Hirano, Yasuo Takeda, Osamu Yamamoto

Department of Chemistry, Faculty of Engineering, Mie University, 1577 Kurimamachiya-cho, Tsu, Mie 514-8507, Japan

HIGHLIGHTS

- Catalytic activity of perovskite-type oxides were examined in LiOH–LiCl electrolyte.
- Chlorine gas was not evolved during charge process.
- These oxides were chemically and electrochemically stable in the electrolyte.

ARTICLE INFO

Article history:
Received 22 May 2012
Received in revised form
31 July 2012
Accepted 10 September 2012
Available online 29 September 2012

Keywords:
Lithium-air battery
Air cathode
Perovskite oxide
Oxygen catalyst

ABSTRACT

Carbon electrodes with perovskite-type oxide catalysts were investigated as air electrodes for aqueous lithium-air secondary batteries. The system consisted of a water-stable lithium electrode, an aqueous solution of saturated LiOH with 10 M LiCl as electrolyte, and a carbon black air electrode with perovskite catalyst additive. The stability, oxygen reduction and oxygen evolution catalytic activity of the $La_{0.6}Ca_{0.4}Co_{0.8}Fe_{0.2}O_3$, $La_{0.8}Sr_{0.2}Fe_{0.8}Mn_{0.2}O_3$, and $La_{0.6}Sr_{0.4}Co_{0.2}Fe_{0.8}O_3$ perovskite-type oxides were examined in the LiOH–LiCl electrolyte. The perovskite-type oxides were stable in this solution and the oxygen reduction and evolution overpotential on the carbon black substrate was decreased by addition of these perovskite-type oxides. No chlorine evolution was observed during the oxidation reaction on carbon black with the perovskite-type oxides in the LiOH–LiCl electrolyte. The results indicate that carbon black with perovskite-type oxide additives is a potential candidate for the air electrode in the aqueous electrolyte lithium-air rechargeable batteries.

1. Introduction

Lithium-air batteries have a high theoretical specific energy of 11,140 Wh kg^{-1} excluding oxygen and 3458 Wh kg^{-1} including oxygen, which is one order of magnitude or more higher than that of conventional batteries. These batteries are attracting increased attention and R&D efforts as possible power sources for electric vehicles. The rechargeable lithium-air battery was first reported in 1996 by Abraham and Jiang [1], which consisted of a lithium metal anode, gel-type polymer electrolyte, and a carbon air electrode with a catalyst, and was the specific energy density was estimated to be 250–350 Wh kg^{-1}. Kuboki et al. reported an extremely high capacity of 5360 mAh g^{-1} (based on carbon mass) for a primary lithium-air cell with a hydrophobic ionic liquid electrolyte [2]. Bruce et al. presented more attractive results for a rechargeable lithium–oxygen cell using an organic electrolyte of 1 M $LiPF_6$ in propylene carbonate and a carbon black air electrode with MnO_2 catalyst, in which a high charge and discharge capacity of 600 mAh g^{-1} (based on carbon mass) was achieved after 50 cycles [3,4].

However, rechargeable lithium-air batteries with non-aqueous electrolytes have some severe problems that must still be addressed, such as lithium metal corrosion by water, CO_2 ingression when operated in air, and high polarization during the charge and discharge process. These problems observed in the non-aqueous system could be solved by employing an aqueous system. The key component of aqueous lithium-air batteries is the water-stable lithium conducting solid electrolyte, because lithium metal reacts severely with water. Recently, a water-stable lithium electrode for lithium-air batteries was proposed by Visco et al. [5] and Imanishi et al. [6]. The water-stable lithium electrode proposed by Imanishi et al. consisted of a lithium metal anode, a polyethylene oxide (PEO)-based lithium conducting polymer electrolyte, and a water-stable lithium conducting solid electrolyte

* Corresponding author. Tel.: +81 59 231 9419; fax: +81 59 231 9478.
E-mail address: imanishi@chem.mie-u.ac.jp (N. Imanishi).

0378-7753/$ – see front matter © 2012 Elsevier B.V. All rights reserved.
http://dx.doi.org/10.1016/j.jpowsour.2012.09.028

of $Li_{1+x+y}Ti_{2-x}Al_xP_{3-y}Si_yO_{12}$ (LTAP), where the polymer electrolyte was used to prevent the direct contact of lithium metal with LTAP, because LTAP is unstable in contact with lithium metal [6]. Aqueous lithium-air batteries with this water-stable lithium electrode should be operated in saturated LiOH aqueous solution, because the cell reaction product is hydrated LiOH, as follows,

$$4Li + 6H_2O + O_2 = 4(LiOH \cdot H_2O). \quad (1)$$

The solubility of LiOH is approximately 5 mol dm^{-3} at room temperature. LTAP is unstable in aqueous solution with a high concentration of LiOH, but stable in saturated LiOH aqueous solution with a high concentration of LiCl [7]. Therefore, in this study, we have examined the performance of the air electrode for oxygen reduction (OR) and evolution (OE) reactions in saturated LiOH aqueous solution with 10 M LiCl (LiOH–LiCl electrolyte).

Bi-functional air electrodes are considered for the development of rechargeable lithium-air batteries [8], where the electrode consumes oxygen during discharge and evolve oxygen during charge. These type of electrodes were developed by Siemens Corp. in the early 1970s for rechargeable zinc-air batteries with a strong alkaline electrolyte and were composed of two layers; a hydrophilic porous nickel sheet adjacent to the electrolyte and a hydrophobic carbon layer bordering the gas phase [9]. The carbon layer plays an active role during the OR reaction, while the nickel layer of the electrode catalyzes the OE reaction. However, nickel cannot be used as the air electrode for aqueous lithium-air batteries, because it is dissolved by the weakly alkaline solution of saturated LiOH with 10 M LiCl during the charging process. Spinel-type oxides such as $NiCo_2O_4$ [10], pyrochlore-type oxides such as $Pb_2Ru_xIr_{1-x}O_{6.5}$ [11], and perovskite-type oxides such as $La_{1-x}Ca_xFe_{0.8}Mn_{0.2}O_3$ [12] have been reported as Bi-functional catalysts for the OR and OE reactions in the strong alkaline solution of the zinc-air battery. In this study, we investigated the catalytic activity of perovskite-type oxides for the OR and OE reactions in LiOH–LiCl electrolyte for use in the air electrodes of lithium-air rechargeable batteries.

2. Experimental

The $La_{0.6}Ca_{0.4}Co_{0.8}Fe_{0.2}O_3$ (LCCF) and $La_{0.8}Sr_{0.2}Fe_{0.8}Mn_{0.2}O_3$ (LSFM) perovskite-type oxides were synthesized using citric acid precursors. The corresponding metal nitrates were dissolved in an aqueous citric acid solution (1 M). The solution was dried at 60 °C until it became viscous. The syrup-like mixture obtained was first heated for 5 h at 60 °C in vacuum and then calcined for 2 h at 700 °C in air. An additional perovskite-type oxide, $La_{0.6}Sr_{0.4}Co_{0.2}Fe_{0.8}O_3$ (LSCF) powder, was purchased from Seimi Chemical Co.

The air electrodes were composed of a reaction layer and an air diffusion layer. The reaction layer was prepared by mixing Ketjen black EC-600JD (KB; Lion Co.) as the carbon substrate, perovskite oxide as the catalyst, and polytetrafluoroethylene (PTFE; 31-JR dispersion, Du Pont-Mitsui Fluorochemicals Co.) as a binder. The weight ratio of KB, catalyst and PTFE was 55:30:15, and the KB to PTFE ratio for the KB electrode without catalyst was 85:15. The electrode mixture was dried for 12 h at 80 °C and then heated to 350 °C to fix the PTFE onto Ti mesh. 0.30 mm thick carbon paper (SIGRACET, SGL Technologies) was attached to the electrode and used as air diffusion layer. The electrode was tested in the LiOH–LiCl electrolyte, the pH value of which was approximately 9. The test cell was equipped with a working electrode (active area of 0.64 cm^2), a platinum plate with a platinum black as a counter electrode, and a Hg/HgO reference electrode. Experiments were carried out at room temperature and sufficient air was supplied using an air pump.

Formation of the perovskite phase was confirmed by X-ray diffraction (XRD; Rigaku, RINT 2000) analysis using Cu Kα radiation. The Brunauer–Emmett–Teller (BET) surface area was measured using a gas adsorption analyzer (Shimadzu Co., Tristar). Cyclic voltammogram (CV) curves were measured using a multichannel potentiostat/galvanostat (Bio Logic, VMP3) at a scan rate of 10 mV s^{-1}. Polarization curves were measured using a potentiostat/galvanostat (Hokuto Denko, HJ-1001SD8). AC impedance spectra were measured using an impedance/gain-phase analyzer (Solartron, 1260) combined with an electrochemical interface (Solartron, 1286) in the frequency range from 1 MHz to 0.01 Hz. All electrochemical measurements were conducted at ambient temperature.

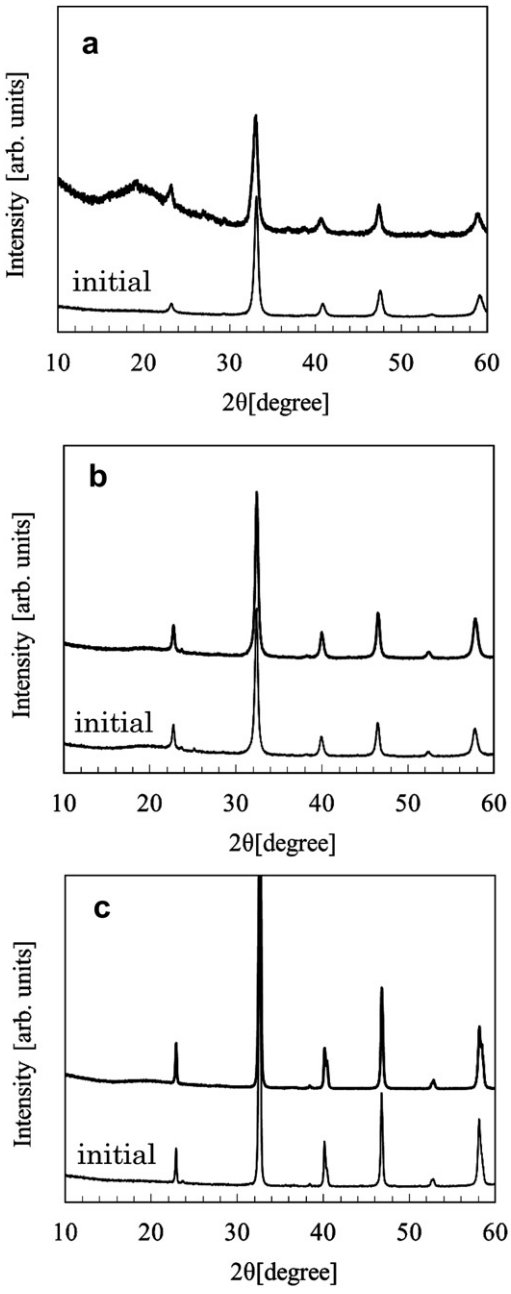

Fig. 1. XRD patterns of (a) $La_{0.6}Ca_{0.4}Co_{0.8}Fe_{0.2}O_3$, (b) $La_{0.8}Sr_{0.2}Fe_{0.8}Mn_{0.2}O_3$ and (c) $La_{0.6}Sr_{0.4}Co_{0.2}Fe_{0.8}O_3$ before and after immersion in saturated LiOH aqueous solution with 10 M LiCl for 7 weeks.

3. Results and discussion

The BET surface areas of LCCF, LSFM, and LSCF were estimated to be 21.0, 24.2, and 1.79 $m^2\ g^{-1}$, respectively. XRD patterns of the synthesized LCCF and LSFM powders and the commercial LSCF powder indicated single phase perovskite-type oxides without impurity phases. Fig. 1 shows XRD patterns of LCCF, LSFM, and LSCF before and after immersion in the LiOH–LiCl electrolyte for 7 weeks at room temperature. No significant change of the XRD profiles was evident as a result of immersion in the solution. A broad peak near 20° in the LCCF pattern is due to the binder used to fix the powder on the sample holder. The XRD analyses indicate that these perovskite-type oxides are stable in the electrolyte used for the present aqueous lithium-air battery.

The important feature of the LiOH–LiCl electrolyte is the electrochemical stability, and in particular, no chlorine evolution during the charge process. The possible air electrode reactions in the solution can be expressed as follows;

$$O_2(g) + 2H_2O + 4e = 4OH^-,\ E^\circ = 0.401\ \text{V vs. NHE}, \quad (2)$$

$$O_2(g) + H_2O + 2e = HO_2^- + OH^-,\ E^\circ = 0.076\ \text{V vs. NHE}, \quad (3)$$

$$\text{and } Cl_2(g) + 2e = 2Cl^-,\ E^\circ = 1.35\ \text{V vs. NHE}. \quad (4)$$

The standard electrode potential of the chlorine evolution reaction is higher than those of the OE reactions. The overpotential for the chlorine evolution reaction is generally low, while that of the OE reaction is high. Therefore, the chlorine evolution reaction may occur for the electrode with the high overpotential for the OE reaction in the alkaline solution. Chlorine is produced commercially by the electrolysis of NaCl aqueous solution using graphite or oxide coated metal electrodes. Fig. 2 shows cyclic voltammograms for the KB electrode and KB electrodes with LCCF, LSMF, and LSCF along with a platinum electrode with platinum black. These voltammograms were recorded between −1.0 and 1.0 V vs. Hg/HgO at a potential scan rate of 10 mV s^{-1} in the LiOH–LiCl electrolyte at room temperature. The open circuit voltage (OCV) for these electrodes in the alkaline solution (pH 9) with a high concentration of chloride ions was dependent on the catalysis of the KB electrode. The OCVs were 0.09 V for KB, 0.11 V for KB with LCCF, 0.04 V for KB with LSCF, and 0.06 V for KB with LSFM vs. Hg/HgO. The OCV values suggest that the main electrode reaction in the LiOH–LiCl electrolyte is the formation of hydroperoxide ions HO_2^- by reaction (3). The change of OCV for the different oxides in the electrode may be due to the difference of catalytic activity for the decomposition of hydroperoxide ions. The CV curve of the platinum electrode shows an anodic current for OE at 0.8 V vs. Hg/HgO, where chlorine evolution was not observed, and a low cathodic current at around −0.1 V vs. Hg/HgO. The anodic currents for the KB and KB/perovskite-oxide electrodes were evident around 0.5 V vs. Hg/HgO. The cathodic currents occurred at −0.1 to −0.2 V vs. Hg/HgO. These electrodes did not show any redox peak before OE in the LiOH–LiCl electrolyte. A similar voltammogram with a single redox peak was

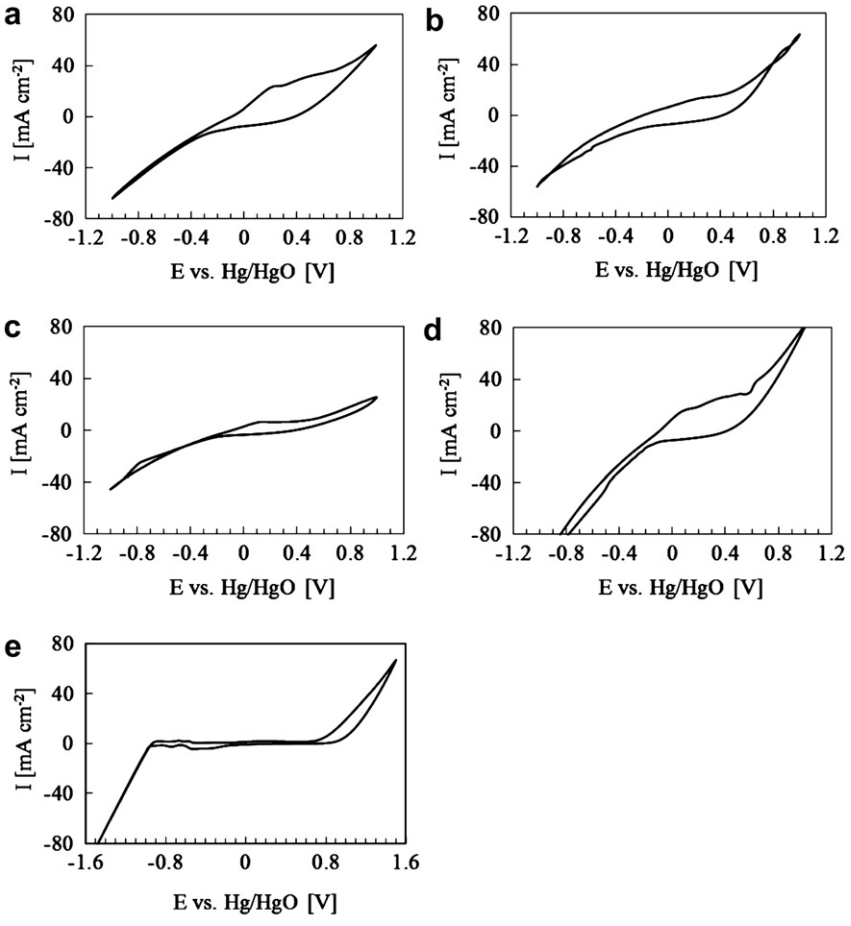

Fig. 2. Cyclic voltammograms of (a) KB, (b) KB with $La_{0.6}Ca_{0.4}Co_{0.8}Fe_{0.2}O_3$, (c) KB with $La_{0.8}Sr_{0.2}Fe_{0.8}Mn_{0.2}O_3$, (d) KB with $La_{0.6}Sr_{0.4}Co_{0.2}Fe_{0.8}O_3$ and (e) Pt plate with Pt black in saturated LiOH aqueous solution with 10 M LiCl measured at room temperature with a scan rate of 10 mV s^{-1}.

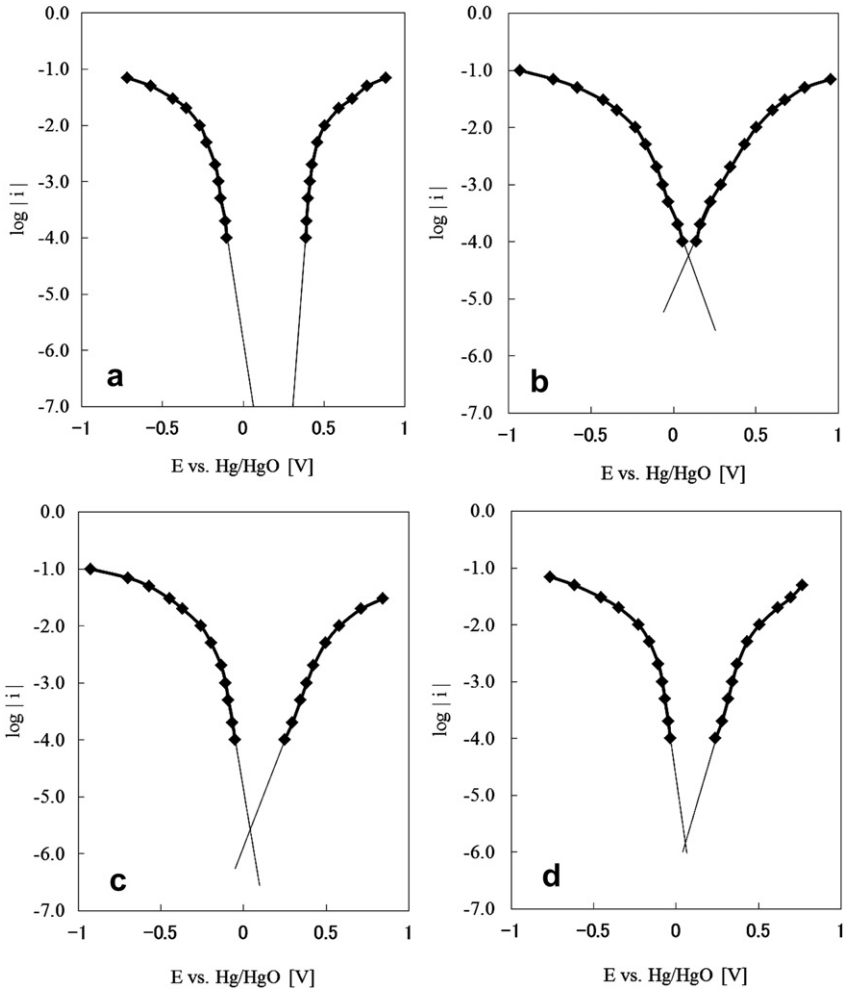

Fig. 3. Polarization curves for (a) KB, (b) KB with $La_{0.6}Ca_{0.4}Co_{0.8}Fe_{0.2}O_3$, (c) KB with $La_{0.8}Sr_{0.2}Fe_{0.8}Mn_{0.2}O_3$, and (d) KB with $La_{0.6}Sr_{0.4}Co_{0.2}Fe_{0.8}O_3$ in saturated LiOH aqueous solution with 10 M LiCl at room temperature.

reported for $La_{0.6}Ca_{0.4}CoO_3$ in 1 M NaOH [13] and for $La_{0.8}Sr_{0.2}CoO_3$ in 1 M KOH [14]. In contrast, $La_{0.8}Ca_{0.2}MnO_3$ exhibited an anodic current due to the oxidation of Mn^{3+} to Mn^{4+}. The OR current on the KB/perovskite oxide electrodes in weak alkaline solution was observed at more negative potential than in the strongly alkaline electrolyte. Thus, the overpotential for the OR reaction in weak alkaline solution is higher than that in strong alkaline solution. We could conclude from the CV studies that the perovskite-type oxides examined in this study are stable for OR and OE reactions in the LiOH–LiCl electrolyte, and that the OE reaction occurs before chlorine evolution.

The OE and OR reaction mechanisms on perovskite-type oxides in strongly alkaline solution were studied extensively by Bockris and Otagawa [15], and Shimizu et al. [13]. In the present study, we have examined the bi-functional performance of perovskite-type oxides in an aqueous electrolyte for use in aqueous lithium-air rechargeable batteries. Potential vs. log current (i) plots of KB, KB with LCCF, KB with LSFM, and KB with LSCF are shown in Fig. 3. The Tafel slopes for OE in the lower overpotential range were 30, 150, 100, and 130 mV decade^{-1} for KB, KB with LCCF, KB with LSFM, and KB with LSCF, respectively. The Tafel slopes of KB with the perovskite-type oxides are comparable to those observed for $La_{0.9}Sr_{0.1}MnO_3$ (125 mV decade^{-1}) and $La_{0.7}Sr_{0.3}FeO_3$ (130 mV decade^{-1}), and higher than that of $La_{0.9}Sr_{0.1}CoO_3$ (66 mV decade^{-1}) in 1 M NaOH aqueous solution [15]. The Tafel slopes for OR in the lower overpotential range for KB, KB with LCCF, KB with LSFM, and KB with LSCF were 50, 130, 50 and 60 mV decade^{-1}, respectively. The exchange current densities for

Table 1
Kinetic parameters for OR and OE on KB with perovskite-type oxides in saturated LiOH aqueous solution with 10 M LiCl at room temperature.

Electrode	Tafel slope (V decade^{-1})		i_{ao} (A cm^{-2})	i_{co} (A cm^{-2})	i_a (A cm^{-2}) at $\eta = 0.3$ V	i_c (A cm^{-2}) at $\eta = 0.3$ V
	OE	OR				
Carbon black (KB)	0.03	0.05	8.4×10^{-16}	2.7×10^{-8}	2.0×10^{-4}	3.6×10^{-3}
$La_{0.6}Ca_{0.4}Co_{0.8}Fe_{0.2}O_3$	0.15	0.13	9.6×10^{-5}	4.0×10^{-5}	4.0×10^{-3}	6.5×10^{-3}
$La_{0.8}Sr_{0.2}Fe_{0.8}Mn_{0.2}O_3$	0.10	0.05	1.0×10^{-6}	2.9×10^{-6}	7.0×10^{-4}	8.2×10^{-3}
$La_{0.6}Sr_{0.4}Co_{0.2}Fe_{0.8}O_3$	0.13	0.06	3.9×10^{-6}	1.2×10^{-6}	1.0×10^{-2}	1.2×10^{-2}

i_{ao}: Exchange current density for the OE reaction.
i_{co}: Exchange current density for the OR reaction.

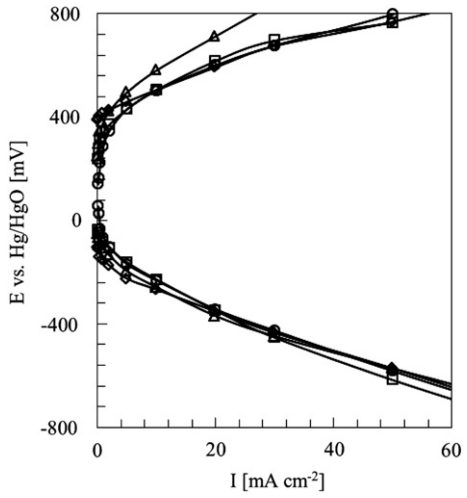

Fig. 4. Polarization curves for (◇) KB and KB with (○) $La_{0.6}Ca_{0.4}Co_{0.8}Fe_{0.2}O_3$, (△) $La_{0.8}Sr_{0.2}Fe_{0.8}Mn_{0.2}O_3$, and (□) $La_{0.6}Sr_{0.4}Co_{0.2}Fe_{0.8}O_3$ in the high current density range.

OR and OE reactions of KB are increased by the addition of the perovskite-type oxides. The highest exchange current density for the OR and OE reactions was observed with the Co-based perovskite-type oxide (LCCF). The Co-based oxide was found to be unstable in alkaline solution [16]. However, stable performance of the oxide can be expected in the LiOH–LiCl electrolyte. The highest current density at $\eta = 0.3$ V was observed for the KB electrode with LSCF. The kinetic data for OE and OR on the KB/perovskite-type oxide electrodes in the LiOH–LiCl electrolyte are summarized in Table 1. The polarization behavior of these electrodes in the higher current density range are compared in Fig. 4. No clear catalytic effect of the pervoskite-type oxide on the electrode reaction was observed in the high current range, but rather the KB with LSFM electrode exhibited a slightly higher overpotential for the OE reaction than the KB electrode without pervoskite-type oxide. The overpotentials for the OR and OE reactions for the KB electrode with LSCF at 20 mA cm^{-2} were 0.39 and 0.58 V, respectively. The overpotential for the OE reaction of the KB electrode with LSFM was almost the same as that of $La_{0.6}Ca_{0.4}CoO_3$ in aqueous 7 M KOH solution, while the overpotential for the OR reaction was higher than that of $La_{0.6}Ca_{0.4}CoO_3$ in 7 M KOH solution [13]. No significant change of the overpotential for the OR and OE reactions on KB with and without addition of perovskite-type oxides suggests that the oxygen gas diffusion process into and from the air electrode may play an important role for the electrode reaction at such a high current density. The overpotential by gas diffusion could be reduced by optimization of the gas diffusion layer design.

The stability of LSCF in the LiOH–LiCl electrolyte was examined after polarization. Fig. 5(a) shows the impedance profile changes of the KB/LSCF electrode with time after polarization at −200 mV vs. Hg/HgO for 24 h. The electrode impedance is decreased just after polarization and then increased to the original value after 5 h. The decrease in the impedance of the electrode may be due to the reduction of Fe^{4+} and/or Co^{4+} to Fe^{3+} and/or Co^{3+}. However, reduced Fe^{3+} and Co^{3+} species were oxidized again to Fe^{4+} and Co^{4+} after a short period in air. Polarization at +400 mV vs. Hg/HgO resulted in no significant change to the impedance profiles, as shown in Fig. 5(b). The XRD patterns of LSCF showed no change after polarization at −200 mV and +400 mV vs. Hg/HgO for 24 h (data not shown), which suggests that the KB electrode with LSCF is stable in the LiOH–LiCl electrolyte for the OR and OE reactions.

Charge–discharge tests of lithium-air cells using the water-stable lithium anode [6], a KB/LSCF air electrode, and the LiOH–LiCl electrolyte were performed at current densities of 0.1–0.3 mA cm^{-2} at 60 °C. The water-stable lithium electrode consisted of lithium metal covered with a lithium conducting polymer electrolyte of PEO with $LiN(CF_3SO_2)_2$ (LiTFSI) and then LTAP. As the electrical conductivity of the PEO_{18}LiTFSI polymer electrolyte is too low to pass an appreciable current at room temperature, the charge–discharge test was carried out at 60 °C, where the polymer electrolyte was amorphous and its conductivity was approximately 10^{-3} S cm^{-1}. The water-stable lithium electrode was prepared by a previously described method [17] using 0.25 mm thick LTAP plate (Ohara, Japan) and 0.2 mm thick PEO_{18}LiTFSI. The conductivity of the LTAP plate was about 1×10^{-3} S cm^{-1} at 60 °C. Fig. 6 shows the typical charge–discharge performance of the Li/PEO_{18}LiTFSI/LTAP/LiOH–LiCl/KB-LSCF air cell at 60 °C. Sufficient air was supplied into the air electrode using an air pump. The electrolyte (ca. 20 μ dm^3) was stored in a separator (Celgard #3501). The open circuit voltage (OCV) was 2.97 V at 60 °C, which is in good agreement with the calculated OCV from reaction (3). Therefore, the reaction product of HO_2^- is stable on the KB/LSCF electrode in the LiOH–LiCl electrolyte. Steady charge–discharge performance was observed in the LiOH–LiCl electrolyte at low current density. However, there was no clear effect of the

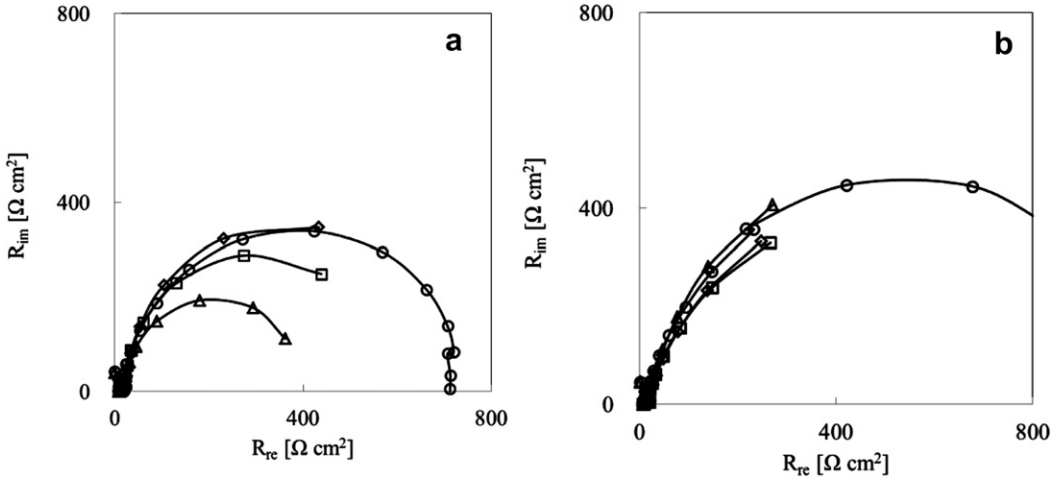

Fig. 5. Time dependence of impedance profiles for KB with $La_{0.6}Sr_{0.4}Co_{0.2}Fe_{0.8}O_3$ in saturated LiOH aqueous solution with 10 M LiCl after polarization at (a) −200 and (b) +400 mV for 24 h: (○) before polarization, (△) just after polarization, (□) after 2 h, and (◇) after 5 h.

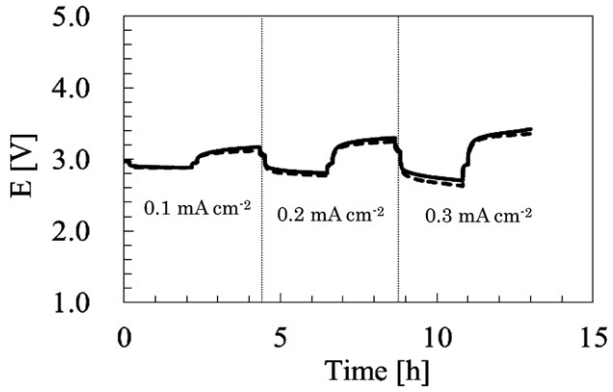

Fig. 6. Charge and discharge curves for Li/PEO_{18}LiTFSI/LTAP/LiCl–LiOH/KB-$La_{0.6}Sr_{0.4}Co_{0.2}Fe_{0.8}O_3$/air (solid line) and Li/PEO_{18}LiTFSI/LTAP/LiCl–LiOH/KB/air (dashed line) cells at 60 °C.

addition of LSCF to the KB electrode on the charge–discharge performance, due to the high polarization at the lithium electrode in the range of the current density examined. The charge–discharge performance of the cell with the KB/LSCF electrode in the LiOH–LiCl electrolyte is slightly poorer than that of the beaker cell with the platinum/platinum black electrode in 1 M LiCl aqueous solution at low current density [6]. The high polarization in alkaline solution at low current density may be due to the formation of peroxide ions. Therefore, to improve the cell performance in the alkaline electrolyte, catalysts for peroxide ion decomposition should be developed.

4. Conclusions

The catalytic activities of LCCF, LSFM, and LSCF perovskite-type oxides for the OR and OE reactions were examined in an electrolyte consisting of saturated LiOH aqueous solution with 10 M LiCl. The OE reaction was observed at 0.5 V vs. Hg/HgO before chlorine evolution. The perovskite-type oxides showed catalytic activity for the OR and OE reactions in the low current density range. In the high current density range, oxygen diffusion was a rate determining step and no clear effect of the catalytic activity of the perovskite-type oxides was observed. A test cell using KB with LSCF as the air electrode and the water-stable lithium electrode was successfully operated in the LiOH–LiCl electrolyte. The results indicate that perovskite-type oxides are attractive catalysts for the air electrode in aqueous lithium-air rechargeable batteries.

Acknowledgements

This study was supported by the Japan Science and Technology Agency (JST) under the project “Advanced Low Carbon Technology Research and Development Program”.

References

[1] K.M. Abraham, Z. Jiang, J. Electrochem. Soc. 143 (1996) 1.
[2] T. Kuboki, T. Okuyama, T. Ohsahi, N. Takami, J. Power Sources 146 (2005) 766.
[3] T. Ogasawara, A. Debart, M. Holzapfel, P.G. Bruce, J. Am. Chem. Soc. 128 (2006) 1390.
[4] A. Debart, A.J. Paterson, J. Bao, P.G. Bruce, Angew. Chem. Int. Ed. 47 (2008) 4521.
[5] S.J. Visco, E. Nimon, B. Katz, L.D. Jonghe, M. Chu, 210th ECS Meeting, Abstract #389.
[6] T. Zhang, N. Imanishi, S. Hasegawa, A. Hirano, J. Xie, Y. Takeda, O. Yamamoto, N. Sammes, Electrochem. Solid-State Lett. 12 (2009) A132.
[7] Y. Shimonishi, T. Zhang, N. Imanishi, D. Im, D.J. Lee, A. Hirano, Y. Takeda, O. Yamamoto, N. Sammes, J. Power Sources 196 (2011) 5128.
[8] T. Zhang, N. Imanishi, Y. Takeda, O. Yamamoto, Chem. Lett. 40 (2011) 668.
[9] L. Calsson, L. Öjefors, J. Electrochem. Soc. 127 (1980) 525.
[10] J. Prakash, D.A. Tryk, W. Aldred, E.B. Yeager, J. Appl. Electrochem. 29 (1999) 1463.
[11] L. Jorisson, J. Power Sources 155 (2006) 23.
[12] Y. Shimizu, A. Nemoto, T. Kyodo, N. Miura, N. Tamazoe, Denki Kagaku 61 (1993) 1458.
[13] Y. Shimizu, K. Uemura, H. Matsuda, N. Miura, N. Yamazoe, J. Electrochem. Soc. 137 (1990) 3430.
[14] S.K. Tiwari, P. Chartier, R.N. Singh, J. Electrochem. Soc. 142 (1995) 148.
[15] J.O'M. Bockris, T. Otagawa, J. Electrochem. Soc. 131 (1984) 290.
[16] T. Hyodo, Y. Shimizu, N. Miura, N. Yamazoe, Denki Kagaku 62 (1994) 158.
[17] T. Zhang, N. Imanishi, A. Hirano, Y. Takeda, O. Yamamoto, J. Electrochem. Soc. 14 (2011) A45.